Long-term ultra-precision phase synchronization technique for locking the repetition rate of OFCs based on FLOM-PD*

ZHOU Weifeng[1,2], HAO Shijie[1,2], CHEN Xing[3], ZHANG Wanpeng[1,2], YUE Zongjie[1,2], and WU Hong[1,2,4]**

1. *College of Electronic Information and Optical Engineering, Nankai University, Tianjin 300350, China*
2. *Tianjin Key Laboratory of Optoelectronic Sensor and Sensing Network Technology, Nankai University, Tianjin 300350, China*
3. *State Key Laboratory of Information Photonics and Optical Communications, Beijing University of Posts and Telecommunications, Beijing 100876, China*
4. *Engineering Research Center of Thin Film Optoelectronics Technology, Nankai University, Tianjin 300350, China*

(Received 29 March 2022; Revised 26 September 2022)

Long-term ultra-precision synchronization between optical frequency combs (OFCs) and microwave oscillators is important for various fields, including scientific observation, smart grid, positioning and navigation, etc. Here, a phase-locked loop system based on fiber loop optical-microwave phase detector (FLOM-PD) is proposed to realize the synchronization of the repetition rate of OFCs and rubidium atomic clocks. Firstly, the scheme and locking process of the system are elaborated, then the mathematical model of the system is established, and the feasibility of the scheme is proved by theoretical analysis and experimental verification. After synchronization, the instability of the system reaches 8.69×10^{-12} at 1 s and 2.94×10^{-13} at 1 000 s, indicating that the phase synchronization system can achieve ultra-precision and stability of OFCs repetition rate.

Document code: A **Article ID:** 1673-1905(2022)12-0712-5

DOI https://doi.org/10.1007/s11801-022-2047-0

With the development of science and technology, high-precision time-frequency synchronization technology is becoming more and more important, which is widely used in scientific observation[1,2], smart grid[3], positioning and navigation[4]. There are three main time-frequency transmission technologies, namely satellite time-frequency transmission, laser time-frequency transmission and optical fiber time-frequency transmission. Among them, with high-precision optical frequency combs (OFCs) and symmetric transceiver path, the accuracy of optical fiber time-frequency transmission is higher than that of laser time-frequency transmission and satellite time-frequency transmission. In addition, optical fiber time-frequency transmission can transmit time reference signal and frequency reference signal at the same time, which has great development potential[5,6].

In practical applications, optical fiber time-frequency transmission needs to synchronize the repetition rate of OFCs with the highly stable frequency references, which is also known as the locking of the repetition rate. At present, the mainstream method is to extract the phase error signals between microwave frequency references and the repetition rate of OFCs through electrical phase detectors, then control the laser piezoelectric ceramics (PZT) expand or contract according to the phase error signals, so as to realize the locking of the repetition rate.

However, the electrical phase detector used in this method will not only affect the accuracy of phase detection, but also bring additional noise in the process of converting optical signals into electrical signals.

In order to solve above problems, an optoelectronic phase-locked loop system based on fiber loop optical-microwave phase detector (FLOM-PD) is proposed to lock the repetition rate of OFCs.

FLOM-PD is an optical-microwave phase detector first proposed by Korean professor Jungwan Kim in 2012, and the structure of FLOM-PD is shown in Fig.1.

With low phase noise and high phase discrimination sensitivity, the FLOM-PD can produce accurate phase error signal and facilitate the precise locking of the mode-locked fiber lasers (MLFLs) and frequency references[7]. The phase detection sensitivity of FLOM-PD is defined as

$$K_{\mathrm{d}} = GRP_{\mathrm{i}}\phi_0, \tag{1}$$

where G is the transimpedance gain of the balanced

* This work has been supported by the National Natural Science Foundation of China (No.U2031208).

** E-mail: wuhong@nankai.edu.cn

detector (BD), R is the responsivity of photodiodes, P_i is the optical power of laser pulse input to FLOM-PD, and ϕ_0 is the modulation depth[8].

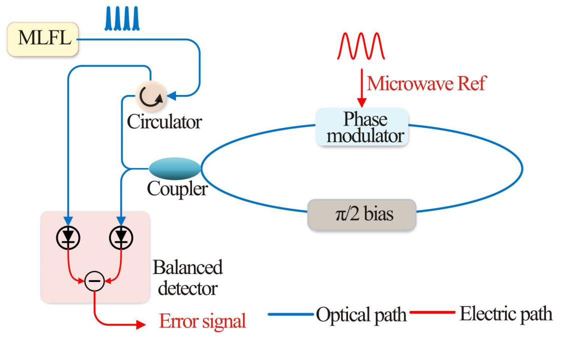

Fig.1 Structure of the FLOM-PD

The structure and phase discrimination sensitivity of FLOM-PD are introduced above. Next, the scheme and locking process of the system based on FLOM-PD will be proposed. The locking process of the system is shown in Fig.2.

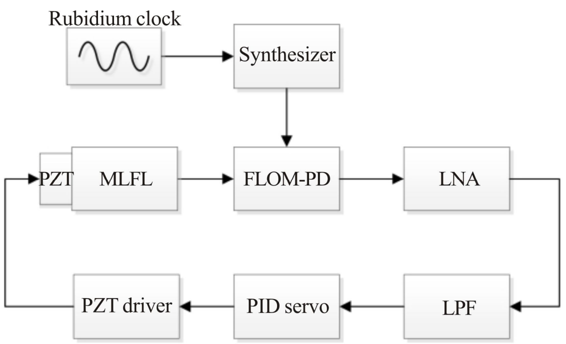

Fig.2 Scheme of the locking system

Firstly, a 1 GHz signal from a synthesizer referenced to a rubidium clock is used as the frequency reference and fed to the FLOM-PD. The MLFL outputs an OFC with a repetition rate of 250 MHz, used as another input of FLOM-PD.

After the two signals are optical-microwave detected by the FLOM-PD, let the extracted error signal successively pass through a low-noise amplifier (LNA), a low pass filter (LPF) and a proportional integral derivative (PID) servo controller, then apply it to a driver to expand or contract the PZT inside the laser, so as to change the cavity length of the MLFL, synchronizing the repetition rate of the OFC and the frequency reference.

In order to better analyze the characteristics of the system shown in Fig.2, this paper simplifies Fig.2 into a time-domain model as shown in Fig.3, then transforms the system from time-domain to S-domain using the Laplace transform. The S-domain model of the system is shown in Fig.4.

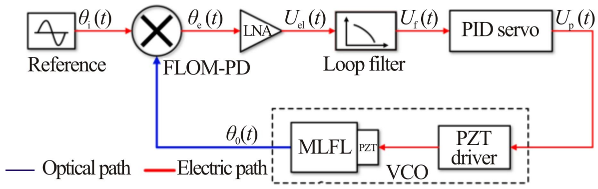

Fig.3 Time-domain model of the system

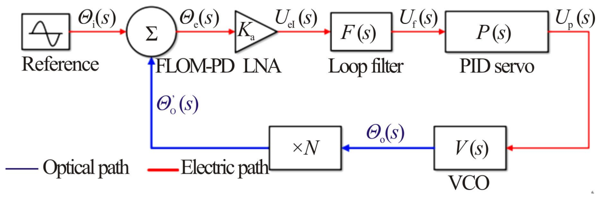

Fig.4 S-domain model of the system

Let $\Theta_i(s)$, $\Theta_o(s)$ and $\Theta_e(s)$ be the Laplace transform of the frequency reference signal $\theta_i(t)$, the laser pulse signal $\theta_o(t)$ and the error signal $U_e(t)$, $U_{e1}(s)$ be the Laplace transform of the signal amplified by the LNA, $U_f(s)$ be the Laplace transform of the output signal from the loop filter, and $U_p(s)$ be the Laplace transform of the output signal after the PID servo. And let K_a be the amplification of the LNA, $F(s)$ be the transfer function of the loop filter , $P(s)$ be the transfer function of the PID controller, and $V(s)$ be the transfer function of the voltage controlled oscillator (VCO).

Then, the open-loop transfer function $G(s)$, closed-loop transfer function $H(s)$ and error transfer function $H_e(s)$ of the system can be defined as

$$G(s)=\frac{\Theta_o'(s)}{\Theta_e(s)}=NK_aF(s)P(s)V(s), \tag{2}$$

$$H(s)=\frac{\Theta_o'(s)}{\Theta_i(s)}=\frac{NK_aF(s)P(s)V(s)}{NK_aF(s)P(s)V(s)+1}, \tag{3}$$

$$H_e(s)=\frac{\Theta_e(s)}{\Theta_i(s)}=\frac{1}{NK_aF(s)P(s)V(s)+1}. \tag{4}$$

In order to perform a detailed analysis of the mathematical model and the locking characteristics of the system, the transfer functions of each part of the system will be analyzed separately in the following.

In the process of modeling the FLOM-PD phase-locked system, the FLOM-PD can be replaced by an ordinary discriminator whose phase discriminative sensitivity is $K_d=GRP_i\phi_0$[9]. Let f_{RF} be the frequency of the reference signal and f_{rep} be the repetition rate of the MLFL, then the frequency of error signal output by FLOM-PD is given by $f_{error}=f_{RF}-Nf_{rep}$, and the Laplace transform of the error signal is

$$\Theta_e(s)=K_d\left[\Theta_i(s)-N\Theta_o(s)\right]=GRP_i\phi_0\left[\Theta_i(s)-N\Theta_o(s)\right]. \tag{5}$$

A third-order LPF as shown in Fig.5 is designed as the loop filter of the system.

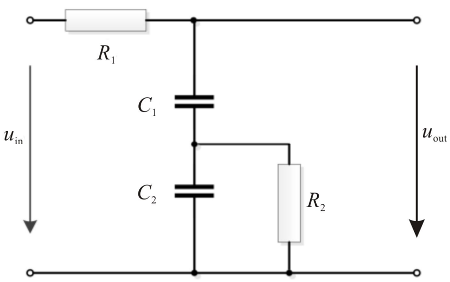

Fig.5 Schematic of the third-order low-pass filter

The transfer function of the filter is

$$F(s)=\frac{s(C_1R_2+C_2R_2)+1}{s^2C_1C_2R_1R_2+s(C_1R_1+C_1R_2+C_2R_2)+1}. \tag{6}$$

To achieve the locking of the repetition rate better, a PID circuit is designed using analog op-amp chips, and the transfer function of the PID servo can be expressed as follows

$$P(s)=K_P+K_I\cdot\frac{1}{s}+K_Ds, \tag{7}$$

where K_P is the proportional coefficient, and K_D and K_I are the integral time and derivative time constants.

The repetition rate of the MLFL can be regulated by PZT driven voltage, which is similar to the voltage controlled oscillator[10]. So as shown in Fig.3, the PZT driver, PZT and the MLFL are replaced by a VCO in the mathematical model. Assume that $V(s)$ is the transmission function of the VCO in the system, which can be approximated as

$$V(s)\approx 2\pi ck_0/sL_0^2, \tag{8}$$

where L_0 is the laser original cavity length, c is the speed of light, and k_0 is the gain of VCO.

After giving the transfer functions of each part in the system, we have analyzed the characteristics of the system as followed.

In the phase-locked system studied in this paper, the final steady-state response is the phase error $\Delta\theta_e(\infty)$ when the system is stable. The calculation of the phase error is generally performed by inputting different excitation signals and calculating the final steady-state error of the system. Typical input signals are phase step signal, frequency step signal, etc. When the input signal $\theta_i(t)$ is given, let its Laplace transform be $\Theta_i(s)$. Using the final value theorem, the phase error signal can be calculated as

$$\Delta\theta_e(\infty)=\lim_{s\to 0}s\Theta_e(s)=\lim_{s\to 0}s\Theta_i(s)H_e(s). \tag{9}$$

When the laser is affected by external influences to occur the phase step of amplitude $\Delta\phi$ and the frequency step of amplitude $\Delta\omega$, substituting the expressions of $H_e(s)$, and the final steady-state error of the system is

$$\Delta\theta_e(\infty)=\lim_{s\to 0}s(\Delta\phi/s+\Delta\omega/s^2)H_e(s)=0. \tag{10}$$

Obviously, after the system has reached the steady state, the phase-locked system is able to quickly eliminate the phase difference and frequency difference between the MLFL and the reference signal through negative feedback, always maintaining the steady state.

Another important characteristic of a phase-locked system is the transient response. Transient response is defined as the response process from the initial input to the final steady state[11]. Based on the error transfer function, the transient response of the system can be obtained for a known excitation signal.

In order to analyze the transient response better, we use MATLAB to simulate the system, then the system parameters are adjusted by simulation and set as Tab.1. The transient response of the system is shown in Fig.6 when the phase step signal and frequency step signal are input to the system respectively.

Tab.1 System parameters for the modeling analysis

Parameter description	Symbol	Value
Laser center wavelength	λ	1 550 nm
Repetition rate of the OFC	f_{rep}	250 MHz
Laser original cavity length	L_0	$c/250\times10^6$
VCO gain	k_0	1×10^{-6}
Phase detector sensitivity	k_d	2.24×10^{-2} V/rad
Parameters of LPF	R_1	50 kΩ
Parameters of LPF	R_2	10 kΩ
Parameters of LPF	C_1	2.24 nF
Parameters of LPF	C_2	22.4 nF
LNA gain	k_a	10
Output RF frequency	f_{RF}	1 GHz

From Fig.6, it's obvious that the system can quickly eliminate the phase jitter and frequency jitter of the VCO and recover to steady state. Both figures also give the transient response at different parameters N. The larger N is, the shorter the convergence time and the more stable the system is. Considering the feasibility and cost, N=4 is finally chosen.

Stability is an important characteristic of a phase-locked system, indicating the ability of maintaining balance. In engineering applications, a common method is to choose a phase margin greater than 45°. When designed for a higher phase margin, it will result in higher stability, slower loop response time and weaker high frequency noise rejection. As shown in Fig.7, the system has a phase margin of about 55°, indicating that the system can work in a stable state.

Based on the above theory analysis, a locking system for the repetition rate of the OFC is constructed as shown in Fig.2.

The direct measurement method is adopted to measure the instability of the OFC. After attenuating the OFC with a repetition rate of 250 MHz output by the MLFL, it is converted into a 250 MHz electrical signal by a photodetector (PD) and measured directly by a frequency counter to obtain the repetition rate after locking, so as to evaluate the frequency instability of the system. The block diagram of the locking and evaluation system is shown in Fig.8. It is worth mentioning that the synthesizer and the frequency counter are synchronized with the rubidium clock.

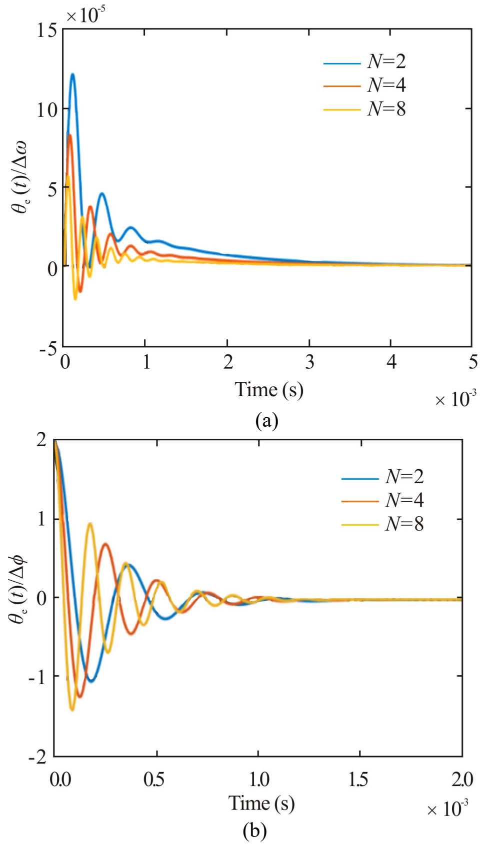

Fig.6 Transient responses of the system to (a) a frequency step and (b) a phase step

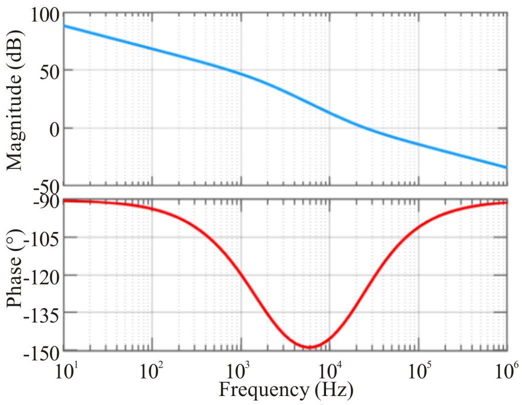

Fig.7 Bode diagram of the system

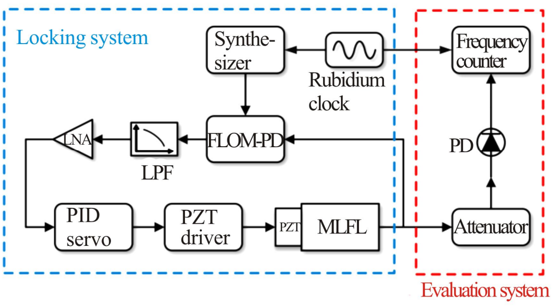

Fig.8 Block diagram of the locking and evaluation system

After locking is achieved, the repetition rates before and after locking are shown in Fig.9. The standard deviation of the repetition rate of the unlocked MLFL is 126.4 Hz, and the standard deviation of the repetition rate of the locked MLFL is 3.02 mHz, which is increased by four orders of magnitude.

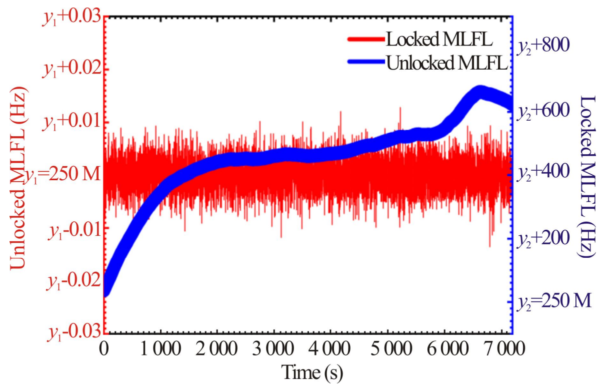

Fig.9 Repetition rates before and after locking

The frequencies of the rubidium atomic clock signal and the unlocked signal of the laser are measured and recorded directly by frequency counter, and then their modified Allan deviations are calculated. The final frequency instability plot of the system is shown in Fig.10.

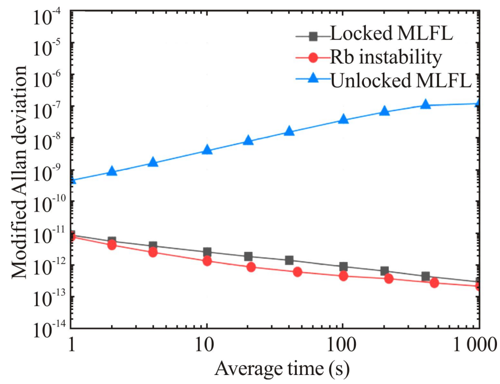

Fig.10 Frequency instability of the locked MLFL, the rubidium clock and the unlocked MLFL

In Fig.10, the blue triangular dotted line shows the frequency instability of the free running laser, the red dotted line shows the frequency instability of the rubidium atomic clock, and the black square dotted line shows the frequency instability of locked MLFL measured after the long-term locking system works stably.

As can be seen, the frequency instability of the unlocked laser is 4.66×10^{-10} at 1 s, and the curve of its frequency instability tends to rise, indicating that its stability is getting worse with the increase of time. In contrast, the frequency stability of the rubidium clock is significantly better than that of the unlocked laser, with the instability of 7.67×10^{-12} at 1 s and 2.17×10^{-13} at 1 000 s.

The instability of the locked MLFL is 8.69×10^{-12} at 1 s and reaches 2.94×10^{-13} at 1 000 s, and the curve of frequency instability shows a continuous decreasing trend as time increases, reflecting the system possesses good long-term stability.

In summary, this paper proposes a phase-locked loop system for synchronizing repetition rate of OFC and frequency reference based on FLOM-PD, establishes a detailed mathematical model, and conducts an experimental demonstration after studying the characteristics of the system. The experimental results show that the instability of the locked repetition rate is 8.69×10^{-12} at 1 s and 2.94×10^{-13} at 1 000 s, which is almost the same as the frequency instability of rubidium atomic clock.

Simulation and experimental results show that the system can achieve long-term ultra-precision phase synchronization of microwave signals and repetition frequencies of OFCs, which can facilitate the development of atmospheric spectroscopy in broadband occultation[12], precision measurements, high-speed optical transmission[13], time-frequency metrology[14] and radio astronomy[15].

Statements and Declarations

The authors declare that there are no conflicts of interest related to this article.

References

[1] KARSHENBOIM S G. Some possibilities for laboratory searches for variations of fundamental constants[J]. Canadian journal of physics, 2000, 78(7)：639-678.

[2] MARION H, DOS S F P, ABGRALL M, et al. Search for variations of fundamental constants using atomic fountain clocks[J]. Physical review letters, 2003, 90(15)：150801.

[3] YANG Y, LI J. Preliminary assessment of the navigation and positioning performance of BeiDou regional navigation satellite system[J]. Science China earth sciences, 2014, 57(1)：144-152.

[4] SUN F, LIU S, ZHU X, et al. Research and progress of Beidou satellite navigation system[J]. Science China information sciences, 2012, 55(12)：2899-2907.

[5] SPRENGER B, ZHANG J, LU Z H, et al. Atmospheric transfer of optical and radio frequency clock signals[J]. Optics letters, 2009, 34(7)：965-967.

[6] DJERROUD K, ACEF O, CLAIRON A, et al. A coherent optical link through the turbulent atmosphere[J]. Optics letters, 2010, 35(9)：1479-1481.

[7] JUNG K, KIM J. Sub-femtosecond synchronization of microwave oscillators with mode-locked Er-fiber lasers[J]. Optics letters, 2012, 37(14)：2958-2960.

[8] JUNG K, KIM J. Long-term stable sub-femtosecond synchronization of microwave signals with mode-locked Er-fiber lasers[C]//2012 IEEE International Frequency Control Symposium Proceedings, May 21-24, 2012, Baltimore, MD, USA. New York：IEEE, 2012：1-4.

[9] ZHANG W, ZHOU W, CHEN X, et al. Development of a photoelectric phase-locked loop model to better synchronize frequency combs and microwaves[J]. Applied optics, 2020, 59(19)：5723-5728.

[10] HOU D, NING B, LI P, et al. Modeling analysis for phase-locking of mode-locked laser[J]. IEEE journal of quantum electronics, 2011, 47(7)：891-898.

[11] ZHANG W, WU H, ZHOU W, et al. Study on ultra-precision phase synchronization technique employing phase-locked loop[J]. Optoelectronics letters, 2021, 17(3)：134-139.

[12] FORTIER T, BAUMANN E. 20 years of developments in optical frequency comb technology and applications[J]. Communications physics, 2019, 2(1)：1-16.

[13] TANG M Z. Research on high-speed optical transmission technology based on optical frequency comb[C]//2020 International Conference on Electrical Engineering and Control Technologies (CEECT), December 10-13, 2020, Melbourne, VIC, Australia. New York：IEEE, 2020：1-6.

[14] MILLO J, ABGRALL M, LOURS M, et al. Ultralow noise microwave generation with fiber-based optical frequency comb and application to atomic fountain clock[J]. Applied physics letters, 2009, 94 (14)：141105.

[15] DOELEMAN S, MAI T, ROGERS A E, et al. Adapting a cryogenic sapphire oscillator for very long baseline interferometry[J]. Publications of the astronomical society of the pacific, 2011, 123(903)：582.